RESEARCH ARTICLE



Investigation of thermal property of plasma-polymerized fluorocarbon thin films

Eunmi Cho^{1,2} | Sehwan Song³ | Mac Kim¹ | Jin-Seong Park² | Sungkyun Park³ Sang-Jin Lee¹ •

Correspondence

Sungkyun Park, Department of Physics, Pusan National University, Busan 46241, Republic of Korea.

Email: psk@pusan.ac.kr

Sang-Jin Lee, Chemical Materials Solutions Center, Korea Research Institute of Chemical Technology (KRICT), Daejeon 34114, Republic of Korea.

Email: leesj@krict.re.kr

Funding information

Korea Basic Science Institute; Korea Research Institute of Chemical Technology; Ministry of Education

Abstract

The physical property changes in the plasma-polymerized fluorocarbon (PPFC) thin films near the melting temperature (T_m) were investigated through chemical structure analysis. The PPFC thin films, produced by semi-crystalline polytetrafluoroethylene (PTFE)-based polymer sputtering target, form amorphous polymers with outstanding properties, such as high water repellency and high optical transmittance, electrical insulation, and chemical resistance. Interestingly, in-situ X-ray photoelectron spectroscopy analysis revealed that the PPFC thin films maintained their physical properties at temperatures above the $T_{\rm m}$ in vacuum and exhibited properties similar to those of bulk PTFE while maintaining amorphous structure. Therefore, this thin film can be applied to various devices and surface coatings manufactured at high temperatures.

KEYWORDS

melting temperature, polytetrafluoroethylene, plasma-polymerized fluorocarbon, sputtering, thermal study

INTRODUCTION

Polymers are widely used basic materials in household items, such as kitchen equipment, packaging containers, and hygiene products, because commodity polymers, such as polyethylene, polypropylene, and polyurethane, are inexpensive and easy to process and mass-produce. Further, it also can be used in high-tech industries, such as the automotive, electric power, electronics, and aerospace industries. However, most commodity polymers have low thermal properties because their glass transition temperatures and melting temperature (T_m) is less than 100°C. In addition, products and parts used in hightech industries are exposed to harsh environments (e. g., high

temperature, high pressure), requiring polymers with high thermal properties, high hardness, and strong chemical resistance.

High-heat-resistant polymer materials are classified as superengineering plastics include polyimide, polyether ether ketone, and fluoropolymer.² Polytetrafluoroethylene (PTFE) is a semi-crystalline fluoropolymer with superb chemical resistance, a low friction coefficient, a low surface energy, and dielectric properties.³⁻⁵ Furthermore, PTFE has remarkable thermal stability owing to its high $T_{\rm m}$ (340°C) and maintains its physical properties over a wide temperature range (-260°C to 260°C); therefore, it is widely used, from industrial machinery to cutting-edge semiconductors and the aerospace industries. 3,6-8 In the coating industry, PTFE is also used as a surface protective film. 9-16 Typically, a protective PTFE film is applied by painting on the surface, heating at a constant temperature. However, owing to the low surface energy of PTFE (e.g., low

Eunmi Cho and Sehwan Song have contributed equally to this work.

This is an open access article under the terms of the Creative Commons Attribution License, which permits use, distribution and reproduction in any medium, provided the original work is properly cited.

© 2022 The Authors. Polymers for Advanced Technologies published by John Wiley & Sons Ltd.

¹Chemical Materials Solutions Center, Korea Research Institute of Chemical Technology (KRICT), Daejeon, Republic of Korea

²Department of Materials Science and Engineering, Hanyang University, Seoul, Republic of Korea

³Department of Physics, Pusan National University, Busan, Republic of Korea

adhesion to the substrate), it is difficult to apply the coating on the various kinds of materials.

Recently, plasma-polymerized fluorocarbon (PPFC) thin films deposition using sputtering processes has considerable attention to replacing conventional PTFE coatings because that the process is an environmental-friendly coating method (unlike a chemical vapor deposition method using toxic gas), capable of fabricating high-quality polymer thin films with a high density in a nanometer-scale thickness. 17-25 In general, radio frequency (RF) sputtering is widely used when thin PPFC thin films are deposited using PTFE targets.²⁶ Recently, a midfrequency (MF) sputtering method has been adopted to deposit PPFC thin films using reactive sputtering with conductive targets instead of using RF sputtering.²⁷ The MF sputtering system typically using 20-80 kHz frequency generator that reduce signal reflection without additional matching box and improves the sputtering efficiency in a reactive sputtering process. In this study, we fabricated composite PTFE targets containing carbon nanotube (CNT) to impart an electrical conductivity to polymer targets and deposited PPFC thin films by using MF sputtering with the CNT-PTFE composite targets.

In general, polymers with a crystallinity of approximately 25% or higher are classified as semi-crystalline polymers. Polytetrafluoroethylene is a semi-crystalline polymer with a relatively high crystallinity (92%-98%).3-5,28 However, PPFC thin films fabricated by sputtering of a bulk PTFE target are amorphous. 19,29,30 The physical properties of PPFC thin films with an amorphous structure exhibit similar to those of PTFE, such as high water repellency,³¹ electrical insulation, chemical resistance, and thermal properties at room temperature. In addition, it has been reported that PPFC thin films produced by sputtering have excellent adhesion to the substrate, good uniformity of nanometerlevel thickness, a smooth surface, high transparency in the visible light region (unlike opaque bulk PTFE), and high hardness and modulus superior to those of bulk PTFE. 29,32-34 These extraordinary properties of PPFC thin films allow extending the usage areas where conventional PTFE coatings cannot be applied, such as flexible displays, solar cells, antireflection coatings for automobile and building glasses, and selfcleaning films.35-37 However, studies on the thermal properties of PPFC thin films fabricated by sputtering of a bulk PTFE target have only been reported up to 300°C, and there are no reports on thermal properties near the $T_{\rm m}$. ^{38,39} Consequently, it is difficult to apply to high-temperature environments. In particular, to apply PPFC thin films to high-tech components (such as displays and semiconductors) that generate significant heat inside the devices, it is essential to understand how the physical properties of PPFC thin films vary with temperature.

In this study, PPFC thin films prepared by MF sputtering of CNT-PTFE targets were treated at 300–400°C (which encompasses the $T_{\rm m}$ of PTFE) to analyze the structural properties, optical properties, and surface wettability at elevated temperatures, and the results were compared with those of bulk PTFE. The chemical structures of the interior and the surface of the thin films near the $T_{\rm m}$ were analyzed by Fourier-transform infrared spectroscopy (FT-IR) and X-ray photoelectron spectroscopy (XPS), respectively, without performing thermal analysis such as thermogravimetric analysis and differential scanning calorimetry. Furthermore, in-situ XPS analysis was performed to examine annealing

environments dependence. As a result, despite structural differences, PPFC thin films had very similar thermal properties to bulk PTFE. Therefore, they can be applied in the high-temperature environments where PTFE coatings are currently applied and in fields requiring high optical transparency and self-cleaning, such as displays and solar cells.

2 | EXPERIMENTAL

2.1 | PPFC thin film and bulk PTFE preparation

The composite targets are comprising CNTs (K-nanos 200P, 5–15 μm powder size, Hanwha Chemical) and PTFE (TF-1750, 25 μm powder size, Dyneon) with a mass weight ratio of 5:95. PPFC thin films were fabricated by MF sputtering. The sputtering chamber was evacuated using mechanical and cryogenic pumps to a base pressure of 5.0 \times 10 $^{-6}$ Torr. The working pressure during sputtering was 1.5 \times 10 $^{-3}$ Torr. Pure Ar gas was used as the sputtering gas, and its flow rate was controlled using a mass flow controller. The distance between the target and the substrate was 240 mm. PPFC thin films were fabricated at a power of 300 W using a dual-cathode MF power supply (PE II, 40 kHz frequency, Advanced Energy). Glass (25 \times 25 mm², 0.7 T, Eagle glass, Corning) and Si wafers (5 \times 10 mm², WSI0PR0029, iTASCO) were used as substrates. For comparison, the bulk PTFE (TF-1750, Dyneon) was also prepared with dimensions of 5 \times 10 \times 1 mm³.

2.2 | Thermal treatment procedure

The bulk PTFE and PPFC/glass samples were placed in a furnace and heated to 300, 320, 340°C, 360°C, 380°C, and 400°C in air. As shown in Figure 1, the temperature was increased at 5°C/min up to the target temperature, where it was maintained for 1 h before it was lowered at 5°C/min to room temperature.

In-situ XPS (AXIS SUPRA, Kratos) was used to investigate the evolution of the chemical bonding structure of the PPFC thin films in vacuum with an increasing temperature. The XPS chamber was evacuated to a base pressure of $\sim\!10^{-8}$ Torr, and Al K $_{\alpha}$ (1486.6 eV) monochromatic X-rays were used with an accelerating power of 225 W. The charge neutralizer was used to cancel the charge of X-ray collision on the thin film surface. The substrate was heated to the corresponding temperature for 1 h under the same conditions as those for the experiments performed in air.

2.3 | Characterization of PPFC thin films after thermal treatment

The transmittance and reflectance of the PPFC thin film coated on the glass substrate were measured using an ultraviolet–visible (UV–Vis) spectrophotometer (U-4100, Hitachi). The water contact angle (WCA) was measured using a contact angle tester (Phoenix 300 Touch, Surface Electro Optics) with 5 μ l deionized water. The surface of the substrate was observed using an optical microscope (VK-X200K,

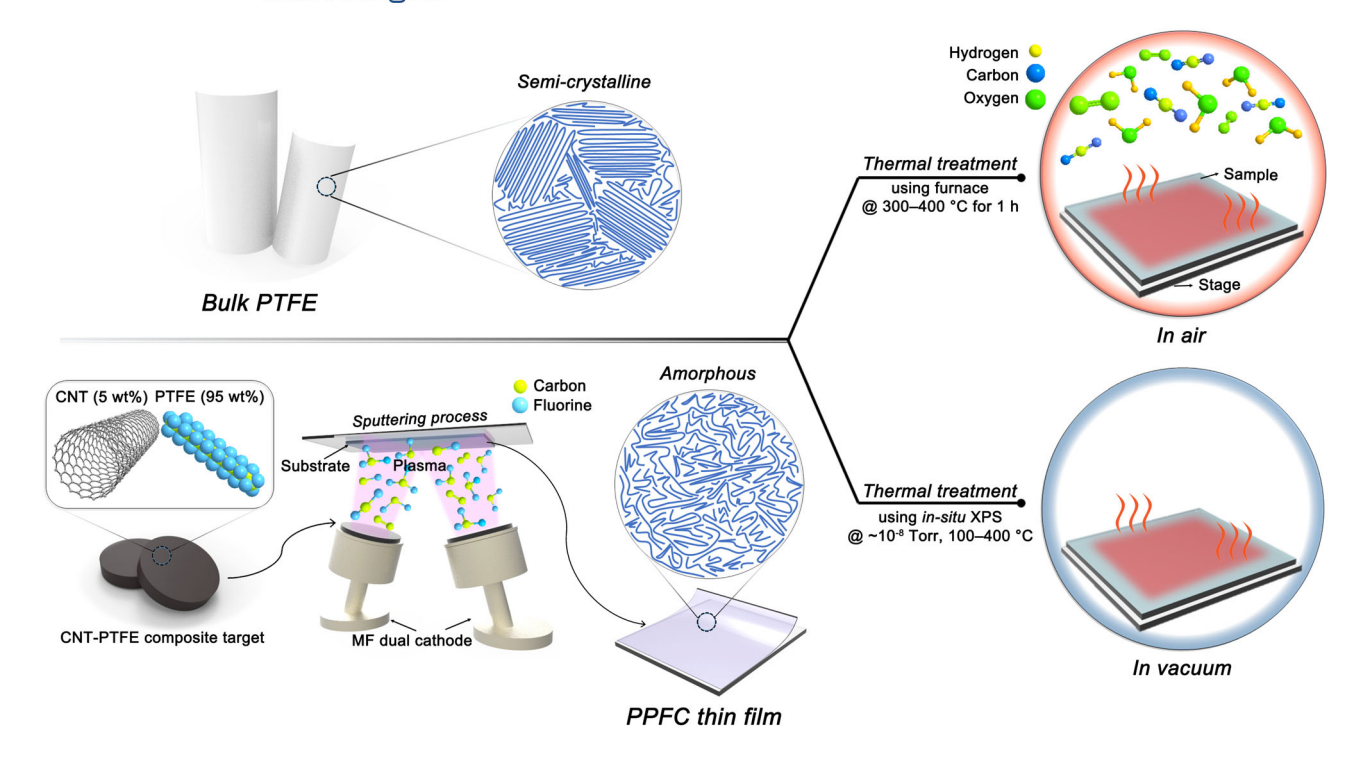


FIGURE 1 Thermal treatment procedure of the bulk PTFE and PPFC thin films

Keyence). The chemical structures of the thermally treated bulk PTFE and PPFC/glass samples were also analyzed by XPS (AXIS NOVA, Kratos). The XPS measurement vacuum degree was 10^{-9} Torr, and the characteristic X-ray was Al-K α (1486.6 eV). X-rays were generated by applying an electric field with an acceleration voltage of 15 keV and an acceleration current of 10 mA. The chemical bonding states of the thermally treated samples were investigated by FT-IR spectroscopy between 400 and 4000 cm $^{-1}$. The bulk PTFE was analyzed in transmission mode (IFS-66/s, Bruker), and a PPFC thin film (1 μ m thick) was coated on an indium tin oxide glass substrate and analyzed in the attenuated total reflectance (ATR, Thermo, Nicolet 5700) mode.

3 | RESULTS AND DISCUSSION

3.1 | Optical properties and surface wettability of bulk PTFE and PPFC thin films after thermal treatment in air

Figure 2 shows the temperature-dependent optical properties and surface wettability of the PPFC thin films in air. For comparison, the properties of glass and Si-wafer substrates were also measured. To maximize the optical transmittance of PPFC thin film in the visible light region, the coating thickness must be equal to $\lambda/4$ (λ is the wavelength of the incident light). Therefore, we deposited the PPFC thin film thickness between 100 and 150 nm. When a PPFC thin film with a thickness of 100 nm was deposited on glass at room temperature, the transmittance increased from 92.0% to 92.6% at a wavelength of 550 nm, and the reflectance decreased from 8.0% to 7.4% owing to the increased transmittance (Figure 2A). This is because the PPFC thin

film had an amorphous structure, which suppressed scattering. Further, because the PPFC thin film had a low refractive index (n=1.38), reflection was minimized by destructive interference between reflected waves, resulting in an index-matching that improved transmittance. When the heat was applied to the sample, the transmittance gradually decreased, and the reflectance increased as the temperature increased. Above the $T_{\rm m}$ of PTFE, the optical properties of the sample returned to those of uncoated glass.

The fluorocarbons in PPFC thin films have a very stable chemical bond because of the high electronegativity of fluorine atoms, giving low surface energy. 42,43 Thus, the PPFC thin films were hydrophobic, and the WCA of the glass substrate increased from 42° to 108° after it was coated with the PPFC thin film, as shown in Figure 2B. However, when the PPFC-coated film was heated near the $T_{\rm m}$ (340°C) in air, the hydrophobicity disappeared, and the surface wettability returned to that of the uncoated glass substrate.

When the temperature reached 400°C, the transmittance decreased, and the optical properties (Figure 2A) returned to those of the uncoated glass substrate; even the hydrophobicity (Figure 2B) disappeared. On the other hand, when the PPFC thin film was coated on the bare Si wafer without heat treatment, the WCA changed from 50° (hydrophilic) to 105° (hydrophobic), as shown in the inset of Figure 2C. After heat-treated in air at 400°C for 1 h, the WCA decreased back to 52° (hydrophilic), indicating that the PPFC thin film seems vaporized. In addition, when the temperature increases, the particles in the PPFC thin film are fused to each other and the space between the particles is reduced, thereby reducing the thickness of the PPFC thin film. 44,45 Therefore, the optical microscope, shown in Figure 2C, confirms that the images of the bare Si wafer and the heat-treated PPFC-coated Si wafer appear identical.

FIGURE 2 Optical properties and surface wettability of PPFC thin films after thermal treatment in air. (A) Transmittance (black) and reflectance (blue) spectra of as-deposited and thermally treated PPFC thin films (550 nm wavelength). (B) Surface wettability of as-deposited and thermally treated PPFC thin films. (C) Optical microscope images of as-deposited and thermally treated PPFC thin films on Si wafers (inset: WCA images of Si wafer samples)

3.2 | Chemical structure analysis of bulk PTFE and PPFC thin films after thermal treatment

3.2.1 | FT-IR analysis (in air)

The chemical bonds in PPFC thin films (amorphous polymers) are expected to break easily, even with low energy, compared to those in bulk PTFE (semi-crystalline polymer) because intermolecular bonds of amorphous are weaker than that of crystalline. Figure 3 and Table 1 compare and analyze the changes in chemical bonding after heating of the bulk PTFE (Figure 3A) and PPFC thin films (thickness: \sim 1 μ m) (Figure 3B) using FT-IR spectroscopy. The three observed peaks (a, b, and c) are assigned as follows: a (1201 cm⁻¹) and b (1145 cm⁻¹) correspond to the symmetric and asymmetric stretching of CF2, respectively, and c (630 cm⁻¹) is a wagging peak of CF_2 . 46-48 It is worth noting that bulk PTFE spectra were calibrated to the peak at 1145 cm⁻¹. PTFE has a high $T_{\rm m}$ and a high creep viscosity; therefore, it does not melt and flow at temperatures higher than the $T_{\rm m}$.⁴⁹ In addition, PTFE particles are sintered like powdered metal, sticking to one another to combine into larger particles.^{8,50} Therefore, the bulk PTFE maintained three peaks at temperatures below and above the $T_{\rm m}$.

The PPFC thin films had more peaks than the bulk PTFE, resulting in complex chemical structures (Figure 3B). The PPFC thin film had a

total of six peaks $(\alpha, \beta, \gamma, \delta, \varepsilon, \text{and } \zeta)$ at room temperature, which were assigned as follows: α (1719 cm⁻¹) corresponds to C=CF₂ or CF=CF₂ vibrations, which indicate the amorphous structure as well as the cross-linked architecture of the PPFC thin film; β (1464 cm⁻¹) corresponds to the asymmetric stretching and rocking deformations of CF₂; γ (1252 cm⁻¹) includes the contributions of the CF and CF₃ bonds formed by the plasma in addition to the contribution of the CF₂ in the PTFE; δ (981 cm⁻¹) corresponds to CF₃ vibrations; ε (827 cm⁻¹) corresponds to the bending of CH bonds; and ζ (739 cm⁻¹) corresponds to CF=O, which suggests the incorporation of contaminants in the film.⁵¹ The detailed positions of the as-deposited PPFC thin film and those for each thermal treatment temperature are shown in Table 2.

Contrary to the expectation that the amorphous PPFC thin film would have a lower thermal properties than that of the bulk PTFE, the peaks of the PPFC thin film were maintained without changes of peak position after thermal treatment for 1 h under the $T_{\rm m}$ (340°C) of bulk PTFE. Although PPFC thin films are amorphous polymers, the atomic concentration of F ions on the surface is \sim 54 at.%, and the F/C ratio is 1.2.29 Theoretically, if the bulk PTFE surface contains only C and F, the atomic concentration of F ions is \sim 69 at.%, and the F/C ratio is 2.2.52 Therefore, the PPFC thin films exhibited thermal properties characteristics similar to the bulk PTFE due to their high F ion content and strong C—C and C—F bonds.

10991581, 2022, 10, Downloaded from https://onlinelibrary.wiley.com/doi/10.1002/pat.5800 by Hanyang University Library. Wiley Online Library on [21/09/2023]. See the Terms and Conditions (https://onlinelibrary.wiley.com

conditions) on Wiley Online Library for rules of use; OA articles are governed by the applicable Creative Commons License

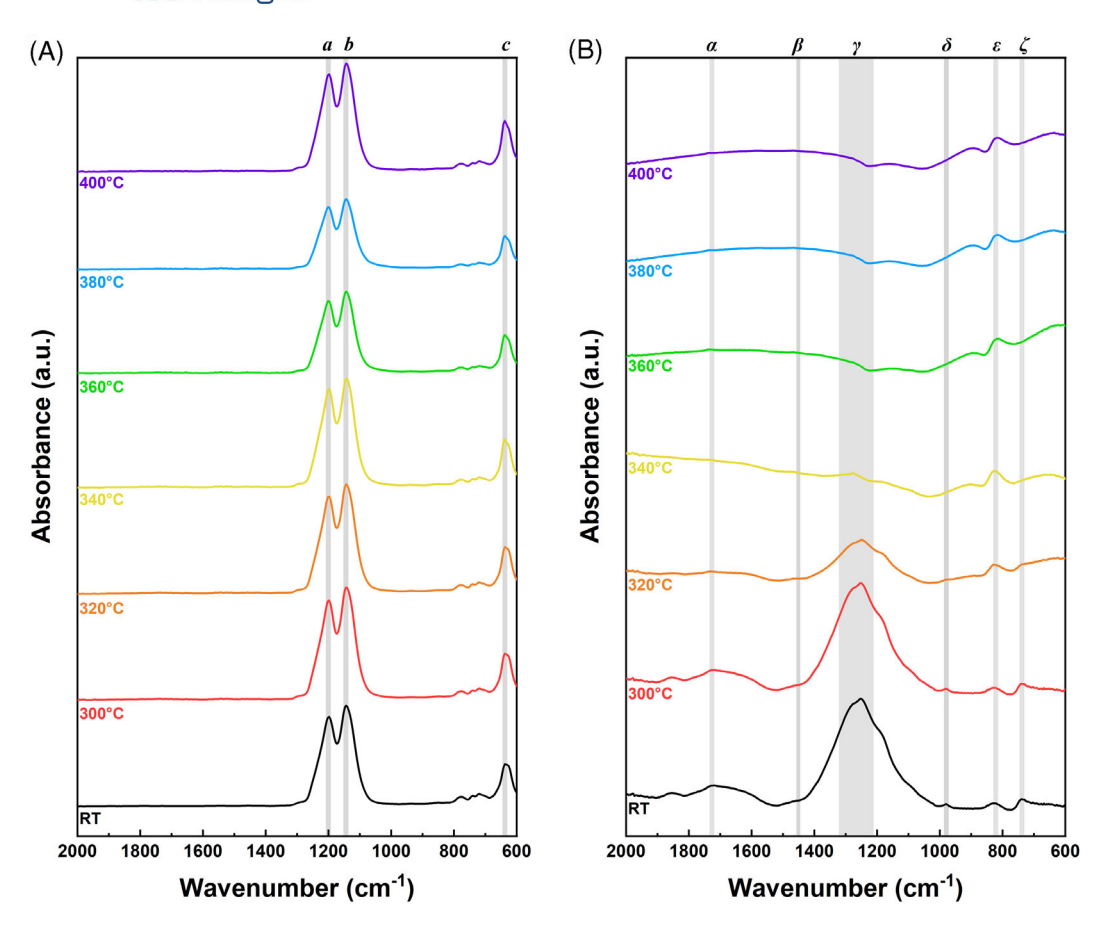


FIGURE 3 FT-IR absorbance spectra of the (A) bulk PTFE and (B) PPFC thin films after thermal treatment in air

	Wavenumber (cm ⁻¹)										
		Bulk PTFE after thermal treatment									
Assignments	Bulk PTFE (20°C)	300°C	320°C	340°C	360°C	380°C	400°C				
а	1201	1201	1201	1201	1201	1201	1201				
b	1145	1145	1145	1145	1145	1145	1145				
С	630	630	630	630	630	630	630				

TABLE 1 FT-IR absorbance peaks for the bulk PTFE after thermal treatment in air

TABLE 2 FT-IR absorbance peaks for the PPFC thin films in the as-deposited and after thermal treatment in air

	Wavenumber (cm ⁻¹)								
		PPFC thin films after thermal treatment							
Assignments	As-deposited PPFC (20°C)	300°C	320°C	340°C	360°C	380°C	400°C		
α	1719	1719	1733	1733	1733	1733	1733		
β	1464	1464	1464	-	-	-	-		
γ	1252	1252	1250	1200	-	-	-		
δ	981	981	978	-	-	-	-		
ε	827	827	827	825	820	818	818		
ζ	739	740	740	-	-	-	-		

However, as the heat treatment temperature increased above the $T_{\rm m}$ of PTFE, the intensity of the α peak gradually decreased for the PPFC thin films. In addition, the peak intensities of the CF₂ bonds (β) present in PTFE and the CF and CF₃ bonds (γ , δ) formed by plasma gradually decreased and then disappeared, indicating that bonds containing F ions disappeared as the temperature increased above the $T_{\rm m}$. In contrast, the peaks of the bulk PTFE were maintained at temperatures higher than the $T_{\rm m}$ (Figure 3A). The chemical bonds (such as CF₃, CF₂, and CF) in the PPFC thin films were dissociated into C and F atoms by thermal energy. These atoms did not recombine into their original state but combined with chemical species such as O or C present in air. This is why the intensities of the bonds containing F ions decreased with increasing temperature and indicating that the PPFC thin film seems vaporized.

3.2.2 | XPS analysis (in air)

Unlike in bulk PTFE, the bonds containing F ions disappeared at temperatures higher than the $T_{\rm m}$ in the PPFC thin films, as shown in Figure 3. The bulk PTFE was 1 mm thick, and the PPFC thin films were approximately 1 μm thick. Consequently, it was difficult to exclude the influence of the film thickness from FT-IR analysis (penetration depth: $\sim\!600$ nm). Therefore, XPS analysis was conducted on the bulk PTFE and PPFC thin films to exclude the influence of thickness and to analyze the chemical bonding state on the surface following heat treatment.

Figure 4 shows the C 1s and F 1s core-level XPS spectra of the bulk PTFE and PPFC thin films. The bulk PTFE spectra were calibrated to the CF₂ binding energy (292.0 eV), and the PPFC thin film spectra were calibrated to the C-C (C-H) binding energy (284.5 eV).²⁹ In the room temperature C 1s spectrum of the bulk PTFE, two peaks appeared corresponding to C-C (C-H) and CF₂ bonds, and the intensity of the CF2 bond peak gradually decreased as the thermal treatment temperature increased (Figure 4A), indicating the F functional group bound to C disappeared as the temperature increased. Similarly, the F-C peak intensity decreases in the F 1s spectra (Figure 4B). In addition, for the bulk PTFE, heat-treated at 360°C, 380°C, and 400°C, a shoulder (red arrow around 294 eV) appeared at the higher the CF₂ binding energy and changed unsystematically (Figure 4A). This variation is related to the changes of the CF_2 bond to a CF_{2+x} bond owing to the thermal treatment. Interestingly, the XPS results differed from the FT-IR results, which did not change with temperature. The distinction might be originated from the different surface sensitivity between XPS (~10 nm) and FT-IR (~600 nm). Therefore, the interior of the bulk PTFE retained the F functional group as the temperature increased because FT-IR can measure a relatively deep region. In contrast, the bulk PTFE exposed on the surface reacted with gases in the atmosphere, causing the F functional group to disappear slightly and C-C, C-O-C, and O-C-O bonds to be formed.

In the C 1s spectrum (Figure 4C) of the PPFC thin film, various peaks appeared, unlike in the bulk PTFE spectrum. For accurate analysis, peak decomposition was performed by fitting the C 1s spectrum at room temperature with Gaussian-Lorentz curves after removing

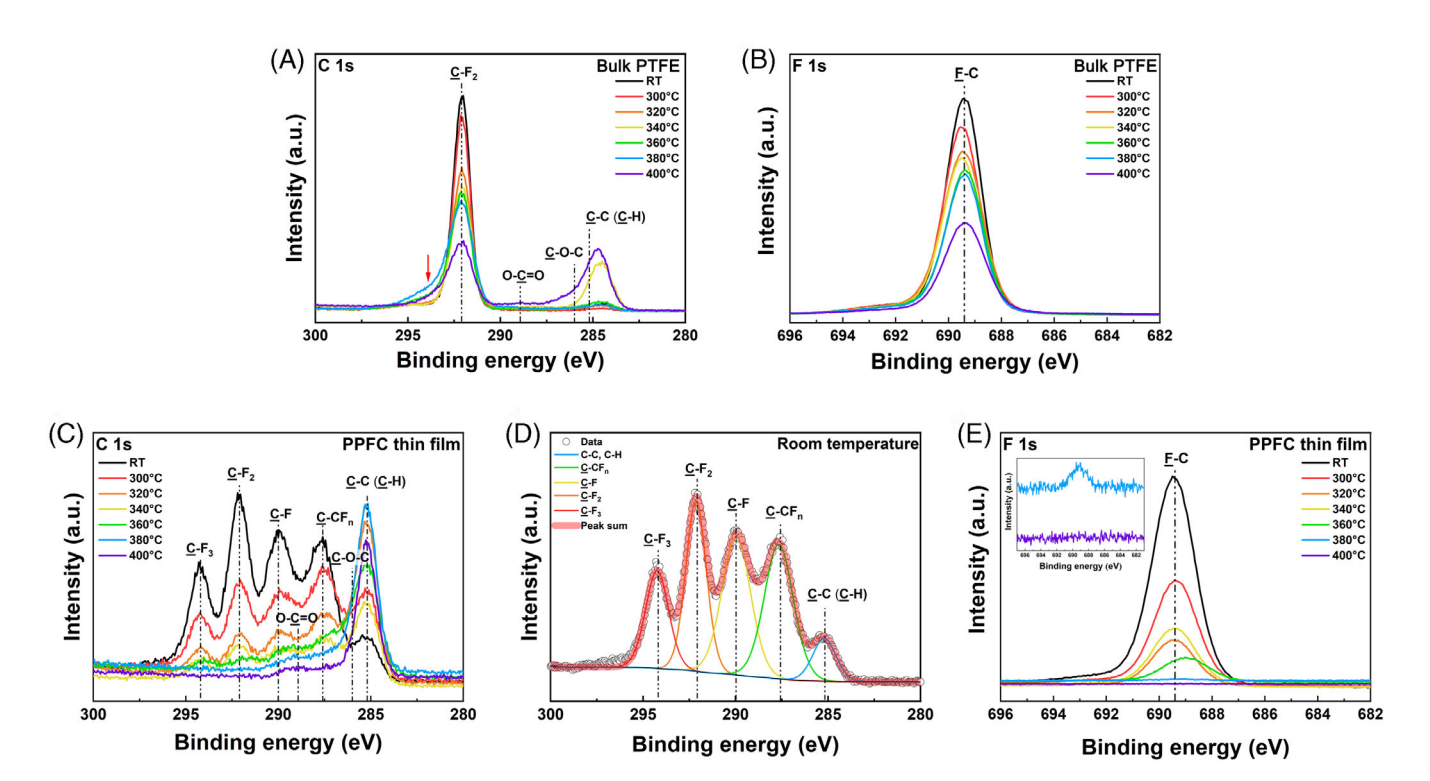
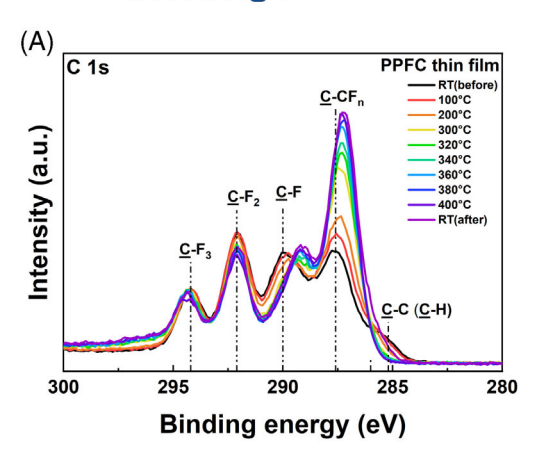


FIGURE 4 XPS spectra of the bulk PTFE and PPFC thin films after thermal treatment in air.(A) C 1s and (B) F 1s spectra of the bulk PTFE, and (C) C 1s spectrum, (D) C 1s spectrum with peak decomposition using Gaussian–Lorentz curves, and (E) F 1s spectrum of the PPFC thin films (inset: magnified XPS spectra of the PPFC thin films heat-treated at 380°C and 400°C)



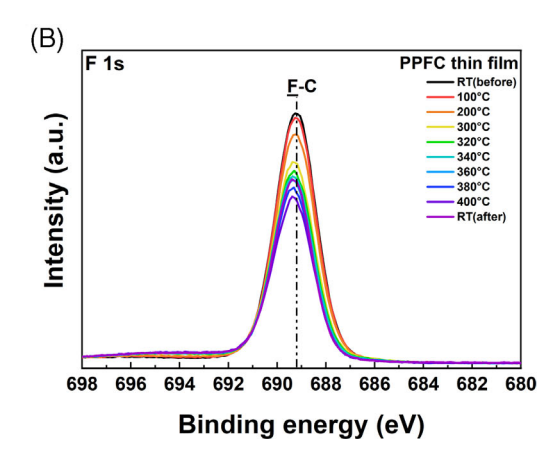


FIGURE 5 In-situ (A) C 1s and (B) F 1s X-ray photoelectron spectra of the PPFC thin film with an increasing temperature in vacuum

the Shirley background, as shown in Figure 4D. 53 The PPFC thin film had five bonds at room temperature: C—C (C—H), C—CF_n, CF, CF₂, and CF₃. Due to surface contamination, the C—C (C—H) bond peak increased as the heat treatment temperature increased. In contrast, the C peaks corresponding to bonds with F gradually decreased. In the thin film heat-treated at 400° C, all the C peaks corresponding to bonds with F disappeared, and only C—C, C—O—C, and O—C=O bonds remained. The same heat treatment dependence was also observed on the bulk PTFE.

For the F 1s spectrum of PPFC thin film (Figure 4E), only one peak with less than 0.5 eV binding energy shift is considered regardless of various binding states with C. As the heat treatment temperature increased, the F 1s peak gradually decreased and disappeared at 360°C or higher. At the same time, the peak moves toward lower binding energy indicate the weakening F-C bond. At 400°C, the F functional group completely disappeared (see inset in Figure 4E). Interestingly, similar to the PPFC thin films, the reduction (not disappearance) of the F functional group was observed on the surface of the bulk PTFE owing to reactions with the chemical species present in air. Interestingly, the reduction, not disappearance, is due to the relatively large volume of the bulk PTFE, which will be the source of extra F. Therefore, that is, when heat is applied above the $T_{\rm m}$, the bulk PTFE and the PPFC thin films are expected to have different thermal properties because of their different structures; however, on the surface or for thin layers, the thermals properties of PPFC thin films and bulk PTFE are the same.

3.2.3 | XPS analysis (in vacuum)

On the surface of the bulk PTFE heat-treated in air, the XPS peak of F bond (C—F₂) decreased, while C—C, C—O—C, and O—C—O bonds were created through reactions with C and O in the atmosphere (Figure 4A). Similarly, for the PPFC thin films, C 1s peak associates with F bonds decreased, whereas reactions with C and O in the atmosphere produced C—C, C—O—C, and O—C—O bonds (Figure 4C). Consequently, it was considered that various gases present in air affected

the chemical state variation of the bulk PTFE and PPFC thin films. Therefore, to specify the effect of the gasses in air, the chemical states of the PPFC thin films were measured by in-situ XPS (i.e., in vacuum heat treatment), as shown in Figure 5.

Figure 5A shows C 1s spectra of PPFC thin film. Similar to the spectra taken in air, the C 1s spectrum was calibrated at 292.0 eV (the CF₂ binding energy) and five bonds such as C-C (C-H), C-CF_n, CF, CF₂, and CF₃ were identified. As the temperature increased, each bond exhibited a different behavior. In air, the strength of the C-C (C—H) bonds increased as the heat treatment temperature increased, whereas in vacuum, the strength of the C-C (C-H) bonds decreased and disappeared completely above 300°C. In addition, in vacuum, the CF₃ and CF₂ peaks did not change significantly with temperature. Furthermore, the CF and C-CF_n bonds slightly shifted toward lower energies and the peak intensity of C-CF_n bonds increased for the in vacuum-treated films. This might be associated with the vaporization of F as the temperature increased, resulting in F vacancies or CF_{1-x} and C-CF $_{n-x}$ bonds formation. The F-defect formation was also confirmed by the decrease in the F 1s peak intensity as the temperature increased. As a result, unlike the film heat-treated in air, F functional group of the film, heat-treated in vacuum, remained above the $T_{\rm m}$ even though the peak energy is shifted to the lower energy due to the F vacancy formation.

In summary, PPFC thin films have excellent optical properties in the visible light region because of their amorphous structure. Simultaneously, they have surface properties similar to those of bulk PTFE and excellent thermal properties considering the in vacuum-treated PPFC thin film. Therefore, it is expected that can be applied in various applications, including those requiring water repellency, antireflection, and high-temperature resistance.

4 | CONCLUSION

The thermal studies of semi-crystalline bulk PTFE and amorphous PPFC thin films were compared and analyzed. The PPFC is a thin film with an amorphous structure produced by sputtering a composite target made by mixing PTFE and CNTs. The $T_{\rm m}$ of the PPFC thin films was confirmed to be approximately 360°C, which is similar to that of the bulk PTFE. However, the surface physical properties of the bulk PTFE were maintained even at temperatures above the $T_{\rm m}$. In contrast, the enhanced optical properties and hydrophobic surface properties of the PPFC thin films disappeared as the temperature increased.

FT-IR analysis from room temperature to near the $T_{\rm m}$ found three peaks for the bulk PTFE (CF₂) and six peaks for the PPFC thin films (CF, CF₂, CF₃, etc.). However, the peaks of the bulk PTFE were maintained above the $T_{\rm m}$, whereas for the PPFC thin films, the peaks corresponding to bonds containing F ions disappeared at 360°C. The surfaces of the bulk PTFE and PPFC thin films showed a gradual decrease in the intensity of the CF₂ bond peaks above the $T_{\rm m}$; in particular, the CF₂ bond changed to the CF_{2+x} bond in bulk PTFE. In addition, it was confirmed that C—C, C—O—C, and O—C—O bonds were formed by reactions with C and O in air on both the bulk PTFE and PPFC thin film surfaces, and the F functional group decreased. This indicates that bulk PTFE and PPFC thin films have the same thermal properties above the $T_{\rm m}$.

In-situ XPS measurements of the PPFC thin films were conducted in vacuum to verify the reaction of the PPFC thin film surfaces with air above the $T_{\rm m}$. In vacuum, C—C, C—O—C, and O—C=O bonds were not formed, even above the $T_{\rm m}$, and the room-temperature chemical structures were maintained without significant changes. Therefore, the surface physical properties changed because the bulk PTFE and PPFC thin films reacted with air at temperatures above the $T_{\rm m}$. In summary, PPFC thin films have excellent optical properties in the visible light region due to their amorphous structure; simultaneously, they have properties similar to those of bulk PTFE and an excellent thermal property.

AUTHOR CONTRIBUTIONS

Sang-Jin Lee and Sungkyun Park conceived the idea and designed the experiments. Eunmi Cho, Mac Kim conducted the PPFC thin film experiments and data analysis. Eunmi Cho and Jin-Seong Park analyzed the chemical bonding states of the bulk PTFE and PPFC thin film by Fourier-transform infrared spectroscopy. Sehwan Song and Sungkyun Park analyzed the chemical structures of the bulk PTFE and PPFC thin film by XPS. Eunmi Cho, Sehwan Song, Mac Kim, Jin-Seong Park, Sungkyun Park, and Sang-Jin Lee wrote the article. All of the authors discussed the results and commented on the article.

ACKNOWLEDGMENTS

This study was supported by the Core Research Project at Korea Research Institute of Chemical Technology (KRICT) (SI-2152-20) funded by the Ministry of Science and ICT, Korea. S. Park was supported in part by NRF Korea (NRF- 2021M3H4A6A02045432) and by Korea Basic Science Institute (National Research Facilities and Equipment Center) grant funded by the Ministry of Education (grant no. 2021R1A6C101A429).

polymers _advanced _WILEY | 3477 technologies

CONFLICT OF INTEREST

The authors declare that they have no known competing financial interests or personal relationships that could have appeared to influence the work reported in this article.

DATA AVAILABILITY STATEMENT

Research data are not shared

ORCID

Sang-Jin Lee https://orcid.org/0000-0001-7554-1037

REFERENCES

- Verpaalen RCP, Engels T, Schenning APHJ, Debije MG. Stimuliresponsive shape changing commodity polymer composites and bilayers. ACS Appl Mater Interfaces. 2020;12:38829-38844.
- Borodulin AS, Kalinnikov AN. Super engineering polyesters: synthesis and performance characteristics. IOP Conf Ser: Mater Sci Eng. 2020; 709:22038.
- Brown EN, Dattelbaum DM. The role of crystalline phase on fracture and microstructure evolution of polytetrafluoroethylene (PTFE). Polymer. 2005;46:3056-3068.
- Gonon P, Sylvestre A. Dielectric properties of fluorocarbon thin films deposited by radio frequency sputtering of polytetrafluoroethylene. J Appl Phys. 2002;92:4584-4589.
- Bunn CW, Howells ER. Structures of molecules and crystals of fluorocarbons. Nature. 1954;174:549-551.
- Jia ZN, Yang YL, Chen JJ, Yu XJ. Influence of serpentine content on tribological behaviors of PTFE/serpentine composite under dry sliding condition. Wear. 2010;268:996-1001.
- Gamboni OC, Riul C, Billardon R, Bose Filho WW, Schmitt N, Canto RB. On the formation of defects induced by air trapping during cold pressing of PTFE powder. *Polymer*. 2016;82:75-86.
- Henri V, Dantras E, Lacabanne C, Dieudonne A, Koliatene F. Thermal ageing of PTFE in the melted state: influence of interdiffusion on the physicochemical structure. *Polym Degrad Stab.* 2020;171:109053.
- Lee MK, Park C, Jang TS, Kim HE, Jeong SH. Enhanced mechanical stability of PTFE coating on nano-roughened NiTi for biomedical applications. *Mater Lett*. 2018;216:12-15.
- Zhang S, Liang X, Gadd GM, Zhao Q. Advanced titanium dioxidepolytetrafluorethylene (TiO₂-PTFE) nanocomposite coatings on stainless steel surfaces with antibacterial and anti-corrosion properties. Appl Surf Sci. 2019;490:231-241.
- Xu P, Jin Z, Zhang T, Chen X, Qiu M, Fan Y. Fabrication of a ceramic membrane with antifouling PTFE coating for gas-absorption desulfurization. *Ind Eng Chem Res.* 2021;60:2492-2500.
- 12. Fan H, Su Y, Song J, Wan H, Hu L, Zhang Y. Design of "double layer" texture to obtain superhydrophobic and high wear-resistant PTFE coatings on the surface of Al_2O_3/Ni layered ceramics. *Tribol Int*. 2019;136:455-461.
- Bandaru AK, Kadiyala AK, Weaver PM, O'Higgins RM. Mechanical and abrasive wear response of PTFE coated glass fabric composites. Wear. 2020;450:203267.
- Price DM, Jarratt M. Thermal conductivity of PTFE and PTFE composites. Thermochim Acta. 2002;392:231-236.
- Liu Z, Zhou B, Rogachev AV, Yarmolenko MA. Growth feature of PTFE coatings on rubber substrate by low-energy electron beam dispersion. *Polym Adv Technol*. 2016;27:823-829.
- Ohkubo Y, Ishihara K, Sato H, et al. Adhesive-free adhesion between polytetrafluoroethylene (PTFE) and isobutylene-isoprene rubber (IIR) via heat-assisted plasma treatment. RSC Adv. 2017;7:6432-6438.

- 17. Biederman H, Ojha SM, Holland L. The properties of fluorocarbon films prepared by rf sputtering and plasma polymerization in inert and active gas. *Thin Solid Films*. 1977;41:329-339.
- 18. Biederman H. RF sputtering of polymers and its potential application. *Vacuum*. 2000;59:594-599.
- Biederman H, Zeuner M, Zalman J, et al. Rf magnetron sputtering of polytetrafluoroethylene under various conditions. *Thin Solid Films*. 2001;392:208-213.
- Zaporojtchenko V, Chakravadhanula VSK, Faupel F, et al. Residual stress in polytetrafluoroethylene-metal nanocomposite films prepared by magnetron sputtering. *Thin Solid Films*. 2010;518:5944-5949.
- Zaporojtchenko V, Podschun R, Schürmann U, Kulkarni A, Faupel F. Physico-chemical and antimicrobial properties of co-sputtered ag-au/PTFE nanocomposite coatings. *Nanotechnology*. 2006;17:4904-4908.
- Schürmann U, Takele H, Zaporojtchenko V, Faupel F. Optical and electrical properties of polymer metal nanocomposites prepared by magnetron co-sputtering. Thin Solid Films. 2006;515:801-804.
- Iwamori S, Hasegawa N, Uemura A. Fluorocarbon polymer thin films prepared by three different types of RF magnetron sputtering systems. Surf Coat Technol. 2008;203:59-64.
- Iwamori S, Tanabe T, Yano S, Noda K. Adsorption properties of fluorocarbon thin films prepared by physical vapor deposition methods. Surf Coat Technol. 2010;204:2803-2807.
- Iwamori S, Noda K. Optical property of fluorocarbon thin films deposited onto polyester film substrate by an RF sputtering. *Mater Lett.* 2012;66:349-352.
- Davidse PD, Maissel LI. Dielectric thin films through rf sputtering. J Appl Phys. 1966;37:574-579.
- Rettich T, Wiedemuth P. High power generators for medium frequency sputtering applications. J Non Cryst Solids. 1997;218:50-53.
- Pace GT, Wang H, Whitacre JF, Wu W. Comparative study of waterprocessable polymeric binders in LiMn₂O₄ cathode for aqueous electrolyte batteries. *Nano Select*. 2021;2:939-947.
- Kim SH, Kim CH, Choi WJ, et al. Fluorocarbon thin films fabricated using carbon nanotube/polytetrafluoroethylene composite polymer targets via mid-frequency sputtering. Sci Rep. 2017;7:1-10.
- Stelmashuk V, Biederman H, Slavinska D, Zemek J, Trchova M. Plasma polymer films rf sputtered from PTFE under various argon pressures. Vacuum. 2005;77:131-137.
- Kim SH, Kim M, Lee JH, Lee SJ. Moisture barrier films containing plasma polymer fluorocarbon/inorganic multilayers fabricated via continuous roll-to-roll sputtering. *Plasma Processes Polym.* 2018;15:1700221.
- Küster S, Ludwig N, Willers G, Hoffmann J, Deising HB, Kiesow A. Thin PTFE-like membranes allow characterizing germination and mechanical penetration competence of pathogenic fungi. *Acta Biomater*. 2008;4:1809-1818.
- Kang TW, Kim SH, Kim M, Cho E, Lee SJ. Highly flexible, hydrophobic, and large area plasma-polymer-fluorocarbon/cu/SiN_x transparent thin film heater and thermotherapy pad application. *Plasma Processes Polym.* 2020;17:1900188.
- Kim SH, Cho E, Kim M, Lee SJ. High-performance rollable polymer/metal/polymer thin-film heater and heat mirror. *Plasma Processes Polym*. 2021;18:2100098.
- Kim M, Kang TW, Kim SH, et al. Antireflective, self-cleaning and protective film by continuous sputtering of a plasma polymer on inorganic multilayer for perovskite solar cells application. Sol Energy Mater sol Cells. 2019;191:55-61.
- Kim SH, Kim M, Lee JH, Lee SJ. Self-cleaning transparent heat mirror with a plasma polymer fluorocarbon thin film fabricated by a continuous roll-to-roll sputtering process. ACS Appl Mater Interfaces. 2018; 10:10454-10460.

- Kang TW, Kim SH, Kim CH, et al. Flexible polymer/metal/polymer and polymer/metal/inorganic trilayer transparent conducting thin film heaters with highly hydrophobic surface. ACS Appl Mater Interfaces. 2017;9:33129-33136.
- Yu Y, Ma Y, Huang X, Song Y, Zhang T, Lu C. Annealing effect on the structure relaxation and mechanical properties of a polytetrafluoroethylene film by RF-magnetron sputtering. Surf Coat Technol. 2021; 405:126591.
- Tripathi S, De R, Haque SM, et al. Annealing dependent evolution of columnar nanostructures in RF magnetron sputtered PTFE films for hydrophobic applications. *Mater Res Express*. 2018;5:015312.
- Cho E, Kim SH, Kim M, Park JS, Lee SJ. Super-hydrophobic and antimicrobial properties of ag-PPFC nanocomposite thin films fabricated using a ternary carbon nanotube-ag-PTFE composite sputtering target. Surf Coat Technol. 2019;370:18-23.
- Cho E, Kim YY, Ham DS, et al. Highly efficient and stable flexible perovskite solar cells enabled by using plasma-polymerizedfluorocarbon antireflection layer. *Nano Energy*. 2021;82:105737.
- 42. Zisman WA. Contact Angle, Wettability, and Adhesion. Advances in Chemistry: 1964:1-51.
- Pagliaro M, Ciriminna R. New fluorinated functional materials. J Mater Chem. 2005;15:4981-4991.
- Jiang Y, Choudhury D, Brownell M, Nair A, Goss JA, Zou M. The effects of annealing conditions on the wear of PDA/PTFE coatings. Appl Surf Sci. 2019;481:723-735.
- Smausz T, Hopp B, Kresz N. Pulsed laser deposition of compact high adhesion polytetrafluoroethylene thin films. J Phys D. 2002;35:1859-1863.
- 46. Krimm S. Infrared Spectra of High Polymers. Springer; 1960:51-172p.
- Kravets LI, Yablokov MY, Gilman AB, Shchegolikhin AN, Mitu B, Dinescu G. Micro-and nanofluidic diodes based on track-etched poly (ethylene terephthalate) membrane. *High Energy Chem.* 2015;49: 367-374.
- Piwowarczyk J, Jędrzejewski R, Moszyński D, Kwiatkowski K, Niemczyk A, Baranowska J. XPS and FTIR studies of polytetrafluoroethylene thin films obtained by physical methods. *Polymers*. 2019; 11:1629.
- Sciuti VF, Melo CC, Canto LB, Canto RB. Influence of surface crystalline structures on DSC analysis of PTFE. *Mater Res.* 2017;20:1350-1359.
- Frick A, Sich D, Heinrich G, Stern C, Gössi M, Tervoort TA. Relationship between structure and mechanical properties of melt processable PTFE: influence of molecular weight and comonomer content. *Macromol Mater Eng.* 2013;298:954-966.
- Satulu V, Ionita MD, Vizireanu S, Mitu B, Dinescu G. Plasma processing with fluorine chemistry for modification of surfaces wettability. Molecules. 2016;21:1711.
- Lojen D, Primc G, Mozetič M, Vesel A. Effect of VUV radiation and reactive hydrogen atoms on depletion of fluorine from polytetrafluoroethylene surface. Appl Surf Sci. 2020;533:147356.
- Végh J. The Shirley background revised. J Electron Spectrosc Relat Phenom. 2006;151:159-164.

How to cite this article: Cho E, Song S, Kim M, Park J-S, Park S, Lee S-J. Investigation of thermal property of plasma-polymerized fluorocarbon thin films. *Polym Adv Technol.* 2022; 33(10):3470-3478. doi:10.1002/pat.5800